Research in Astron. Astrophys. **2011** Vol. **11** No. **6**, 692–700
http://www.raa-journal.org *http://www.iop.org/journals/raa*

Research in Astronomy and Astrophysics

Magnetic field changes associated with three successive M-class solar flares on 2002 July 26 *

Pu Wang[1], Ming-De Ding[1], Hai-Sheng Ji[2] and Hai-Min Wang[3]

[1] Department of Astronomy, Nanjing University, Nanjing 210093, China; *puwang@263.net*
[2] Purple Mountain Observatory, Chinese Academy of Sciences, Nanjing 210008, China
[3] Space Weather Research Lab, Center for Solar Terrestrial Research, New Jersey Institute of Technology, Newark, NJ 07102, USA

Received 2010 September 21; accepted 2011 January 12

Abstract With an extensive analysis, we study the temporal evolution of magnetic flux during three successive M-class flares in two adjacent active regions: NOAA 10039 and 10044. The primary data are full disk longitudinal magnetograms observed by SOHO/MDI. All three flares are observed to be accompanied by magnetic flux changes. The changes occurred immediately or within $1 \sim 10$ minutes after the starting time of the flares, indicating that the changes are obvious consequences of the solar flares. Although changes in many points are intrinsic in magnetic flux, for some sites, it is caused by a rapid expansion motion of magnetic flux. For the second flare, the associated change is more gradual compared with the 'step-function' reported in literature. Furthermore, we use the data observed by the Imaging Vector Magnetograph (IVM) at Mees Solar Observatory to check possible line profile changes during the flares. The results from the IVM data confirm the flux changes obtained from the MDI data. A series of line profiles were obtained from the IVM's observations and analyzed for flux change sites. We find that the fluctuations in the width, depth and central wavelength of the lines are less than 5.0% even at the flare's core. No line profile change is observed during or after the flare. We conclude that the magnetic field changes associated with the three solar flares are not caused by flare emission.

Key words: Sun: activity — Sun: magnetic field — Sun: flares

1 INTRODUCTION

It is now well known that a solar flare is the result of a rapid release of magnetic energy due to magnetic reconnection. Therefore, studying the evolution of the Sun's magnetic field covering solar flares has always been an important topic in solar physics. However, the triggering mechanism of flares is still not well understood. In recent years, the rapid magnetic changes associated with flares have attracted much more attention (e.g. Wang et al. 2009). For the famous 2000 July 14 'Bastille Day Flare,' Kosovichev & Zharkova (2001) reported a rapid decrease in the strength of the magnetic field associated with the flare. In most cases, these sudden changes were highly unbalanced, challenging conventional pictures of flux emergence or magnetic flux cancelation, in which, theoretically, both the positive and negative magnetic flux should increase or decrease at the same time.

* Supported by the National Natural Science Foundation of China.

Spirock et al. (2002) found a significant increase in magnetic flux of leading polarity after an X20 flare, the largest flare in the last few decades. However, no obvious changes were observed in the magnetic flux of the following polarity. They explained the observed changes as the result of a new flux emergence and/or a change in direction of the field from being more vertical to being more tangential. Wang et al. (2002) summarized the study of six X-class flares and found that unbalanced, sudden and permanent flux changes might be a common property of major solar flares. The phenomenon was further verified with more thorough statistical work by Sudol & Harvey (2005). Wang & Liu (2010) recently summarized the studies of many events and found a tendency that, close to the flaring polarity inversion line, the magnetic fields become more horizontal, consistent with what was predicted by Hudson et al. (2008).

The above mentioned investigations of flare-associated magnetic changes may be incomplete due to the following reasons: 1) the majority of flares studied in literature are large flares, i.e., most of them were X-class. Therefore, only rapid (step-function-like) changes or changes of a significant magnitude have been reported. Changes of a smaller magnitude may exist for smaller flares. 2) A more important issue is that the shape of line profiles, which may be affected by quite different physical conditions found at flaring sites compared to quiet regions, may quantitatively affect the measured magnetic field (Ding et al. 2002; Qiu & Gary 2003; Zhao et al. 2009). This can cause so-called magnetic transience during flares. Thus, it is essential to have line profile information during rapid magnetic flux changes.

In this paper, we report abrupt magnetic flux changes associated with three successive M-class flares on 2002 July 26 in the active regions NOAA 10039 and 10044. We divide the active regions into a number of small boxes and determine the detailed timing of the evolution of magnetic flux in the course of the three flares. In addition, for the first time, we analyze spectral line profiles of a flaring region where an abrupt flux change occurs.

2 THE EVENTS AND DATA

The events for this paper are the three flares that occurred in the active regions NOAA 10039 and 10044 on 2002 July 26 (Table 1).

Table 1 Overview of the Flares

Number in this paper	Starting Time (UT)	Peak Time (UT)	Ending Time (UT)	Number of Hα ribbons	Flare size	Accompanying phenomenon
1	18:57	19:03	19:06	1	M1.0	An Hα surge
2	20:51	21:12	21:29	3	M8.7	A Halo CME
3	22:03	22:17	22:32	2	M4.6	

The GOES-10 $1-10$ Å light curve for the flares is presented in Figure 1. The flares manifested different topologies in their Hα images. The first flare (M1.0) is a small two-ribbon flare occurring in NOAA 10039 (Zhou & Ji 2009). In Hα, it appears as a very compact event. It is an impulsive flare as seen from the GOES light curve. The flare was accompanied by an Hα surge, in which a straight ejection of material occurred with a peak speed of $\sim 110\,\mathrm{km\,s^{-1}}$. The other two flares occurred in NOAA 10044, approximately 150 arcsec southeast of the first flare site. They occurred in a common polarity inversion line in the magnetograms. All the events are two-ribbon flares, with a remote brightening. The second flare (M8.7) is more gradual in soft X-ray and is most probably associated with a halo coronal mass ejection (CME). Wang et al. (2004) studied the vector magnetic fields of this flare using data taken at the Big Bear Solar Observatory (BBSO) and found that a rapid emergence of transverse magnetic flux was associated with it.

The primary data used in this study are full disk longitudinal magnetograms, with one minute cadence, observed by the Michelson Doppler imager onboard the *Solar and Heliospheric Observatory*

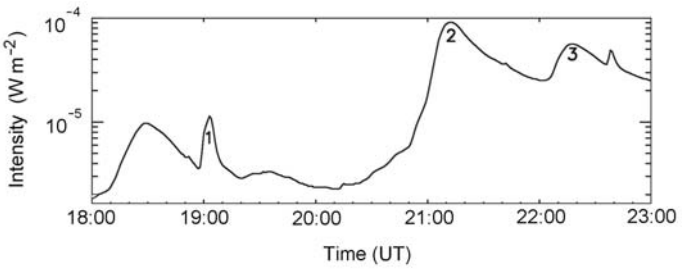

Fig. 1 GOES-10 soft X-ray (1–10 Å) time profile for the three M-class flares, which are numbered 1-3.

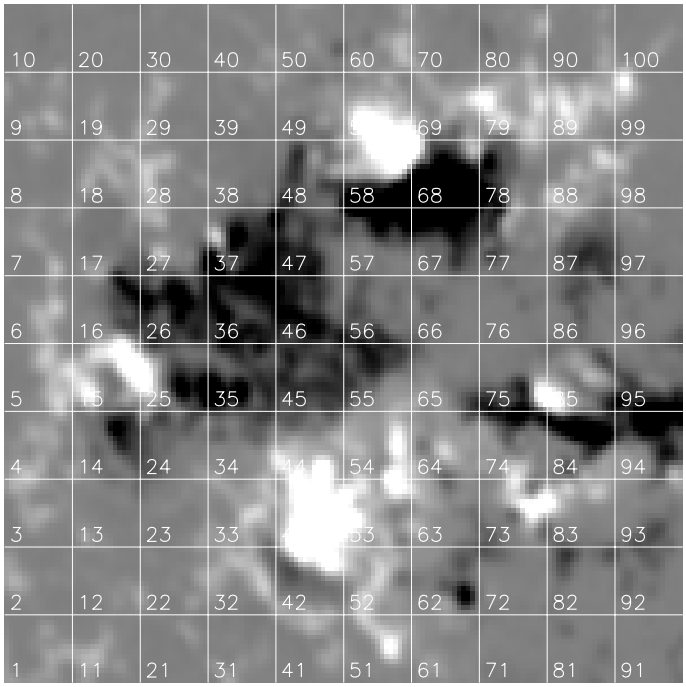

Fig. 2 Divided areas for computing the mean values of both the positive and negative magnetic fields (magnetic flux).

(*SOHO*/MDI; Scherrer et al. 1995). In order to find flaring regions, where line profiles are most likely to change, we use Hα full disk images observed at the BBSO. Hard X-ray maps observed by the Reuven Ramaty High Energy Solar Spectroscopic Imager (*RHESSI*) (Lin et al. 2002) are overlaid on Hα images. Data observed by the Imaging Vector Magnetograph (IVM) (a Stokes polarimeter) at the Mees Solar Observatory (Mickey et al. 1996) are used to obtain magnetograms and line profile information during the flares. The IVM data only provided good coverage of the second flare.

In this paper, we focus on searching for magnetic field changes in every sub-area in the active regions. We divide the magnetograms of the active region into a number of small rectangular regions (Fig. 2), and obtain time profiles of the mean value of the positive and negative magnetic fields for each region. The window size chosen for the sub-regions is fairly arbitrary, but it is sufficiently smaller than the entire active region and sufficiently larger than one pixel. This allows us to observe all sub-areas where there are flare-associated magnetic flux changes, including those with small magnitudes. Several dividing methods have being tried and the results are similar. In this paper, we choose 10×10 as the window size. The time period for calculating the magnetic flux time profiles is from 18:00 to 22:59 UT on 2002 July 26.

3 RESULTS

3.1 The M1.0 Flare

For this flare, Tan et al. (2006) reported a flare-associated rapid drop of longitudinal electric currents and rapid magnetic flux changes. Zhou & Ji (2009) provided extensive multi-wavelength analysis of the flare. They found that the magnetic shear was enhanced immediately after the flare. They also found that flare shear of this event significantly increased followed by a fluctuated decrease, showing a joint process of buildup and relaxation of the sheared magnetic field. The rapid magnetic flux changes are found in box 75 (Figs. 2 and 3). The box is co-spatial with the Hα ribbon. Both positive and negative magnetic fluxes underwent abrupt changes (Fig. 4a and 4b). In Figure 4, the vertical dotted lines mark the starting time of the flares, while the dashed lines mark the peak times for the flares as determined from the GOES soft X-ray light curve. In box 75, the positive magnetic flux shows a sudden decrease of $\sim 5.0 \times 10^{19}$ Mx, while the negative flux exhibits a sudden increase of nearly the same magnitude. The changes occurred one-two minutes after the onset of the flare. It is worth noting that the magnetic flux change in this box is unbalanced. The change occurred within three minutes, causing the time profiles from Tan et al. (2006) to appear like a step-function. The abrupt changes are caused by the rapid emergence of a small leading satellite sunspot.

3.2 The M8.7 and M4.6 Flares

For the second flare, there were three Hα ribbons in total (R1, R2 and R3 in Fig. 3c). The *RHESSI* clean map constructed during 21:25:00$-$21:25:40 shows one single HXR source, which was not co-spatial with any of the flare's Hα ribbons (Fig. 3c). The sudden magnetic flux changes associated with this flare occurred in boxes 33 and 44 (Figs. 2 and 3). The location of box 44 is across the region of the magnetic polarity inversion line. The box is partially co-spatial with both ribbons R1 and R2. Box 33 is partially co-spatial with ribbon R1 and the HXR source (Fig. 3c). In box 44, both positive and negative magnetic fluxes underwent abrupt changes (Figs. 4c and 4d). The positive flux increased, while the negative flux decreased after the onset of the flare. It is worth noting that the sudden change began to occur at the starting time of the flare (within the one minute time resolution). Notably, the changes are more gradual compared with the step-function-like changing behavior of the first flare. The magnetic flux in box 33, which is located in a positive polarity region, also underwent a sudden change. The change in box 33 occurred nearly 10 minutes after the onset of the flare. The change is also gradual.

With vector magnetograms observed at the BBSO, Wang et al. (2004) reported rapid changes of longitudinal magnetic flux in box 33. For box 44, they only reported rapid changes in the transverse magnetic flux.

MDI uses the Ni 6768 Å line to measure the magnetic field (Scherrer et al. 1995). The absorption line originates from the photosphere. With MDI data, there is no information available for the profile of this line which has good spectral resolution. As an important supplementary study, we use the data obtained by the IVM, which can provide simultaneous Stokes I, Q, U, and V profiles at the

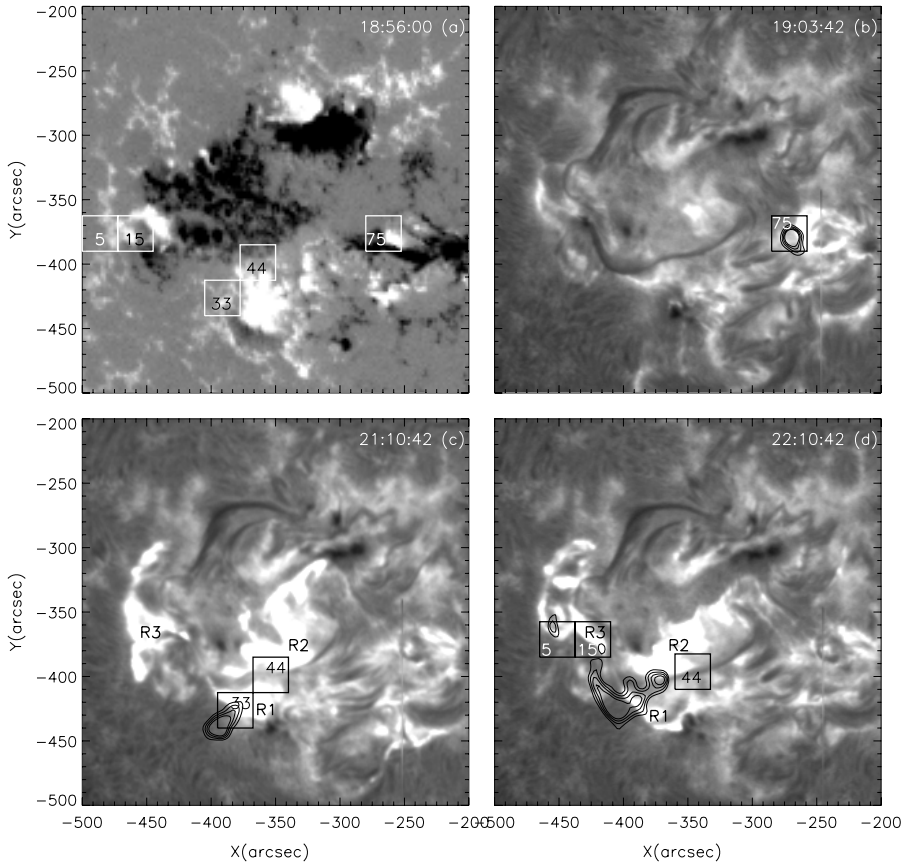

Fig. 3 (a) A map of the MDI magnetogram at 18:56:00 UT is overlaid with the five boxes, where abrupt flare-associated magnetic changes have occurred. (b) Hα image of flare 1 showing one compact ribbon. (c) Hα image of flare 2 showing three ribbons: R1, R2 and R3. (d) Hα image of flare 3 showing two ribbons: R1 and R2. The overlaid contours in the Hα images are from *RHESSI* clean maps in the energy band $25 - 50$ keV.

Fe I 6302.5 Å with 7 pm (pico-meter) wavelength resolution (Mickey et al. 1996). The absorption line, Fe I 6302.5 Å , also originates from the photosphere.

The IVM's observations provided coverage from 20:41 to 21:36. We used the software developed by LaBonte et al. (1999) to produce magnetograms, as well as line profiles. Figure 5a displays a typical longitudinal magnetogram. Based on the magnetograms, we calculated the time profile of the mean magnetic field in boxes 33 and 44 during this period. After removing a systematic error of $\sim$30 G, the results are overlaid on Figure 4c-e with a number of scattered '+' symbols. It can be seen that the trend of the points is in good agreement with the result using MDI magnetograms.

We searched all possible line profile changes in boxes 44 and 33 covering the flare. The line profiles at each point were obtained by averaging over nine pixels centered at this point. We did not find any big changes such as line reversal or obvious line center shifting. As an example, Figure 5a plots a series of line profiles at a point in box 33 (Fig. 5b), which is co-spatial with a flaring kernel. With Gaussian fitting, we obtained the width, depth and center position of the lines. The time profiles

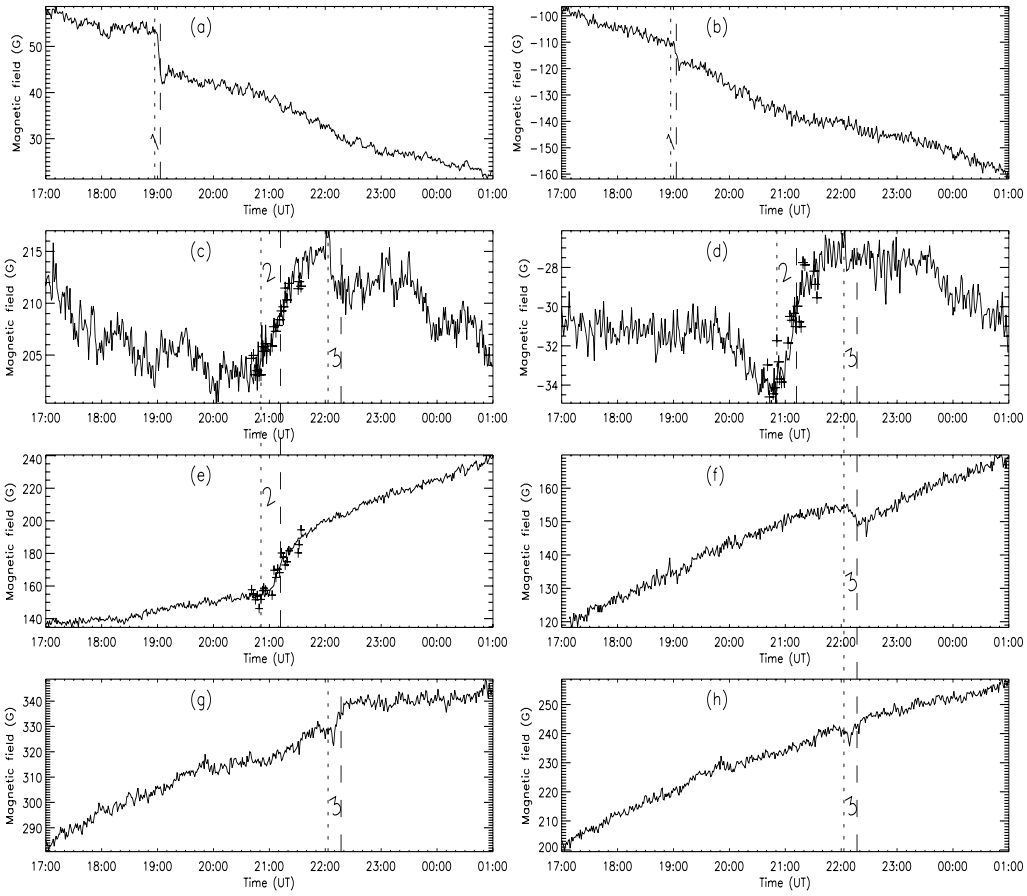

Fig. 4 *Solid lines*: time profiles for the mean magnetic field in different boxes. Panels (a) and (b) are for box 75, panels (c) and (d) are for box 44, panel (e) is for box 33, panel (f) is for box 5, panel (g) is for box 15 and panel (h) is for boxes 5 and 15. The time profiles of magnetic flux in boxes 44 and 33 obtained from IVM data are overlaid with "+" signs in Panels (c)–(e) (20:41 to 21:36 UT).

of the width and depth of the lines, which are normalized to the values of the non-flaring region, are given in Figure 5c-d. Both time profiles show no obvious change. The fluctuation is within 5%. According to the weak field approximation (e.g., Jefferies & Mickey 1991), the upper limit of possible field change corresponding to the measurement error of Mees's line profile should be the same magnitude as the fluctuations of line width and depth. The time profile for the central wavelength of the point in box 33 is plotted in Figure 5e. We can see that the fluctuation is within ± 0.01 Å.

For the third flare, there are also three Hα ribbons (R1, R2 and R3 in Fig. 3d). We constructed a *RHESSI* clean map of its impulsive phase (22:06:50–22:07:30). The contours from the main HXR source were not co-spatial with either of the Hα ribbons, except that some weak HXR emissions appear from ribbon R3. Again, in box 44, sudden magnetic changes associated with this flare occurred for both positive and negative fluxes (Figs. 4c–d). As mentioned above, in box 44 there were

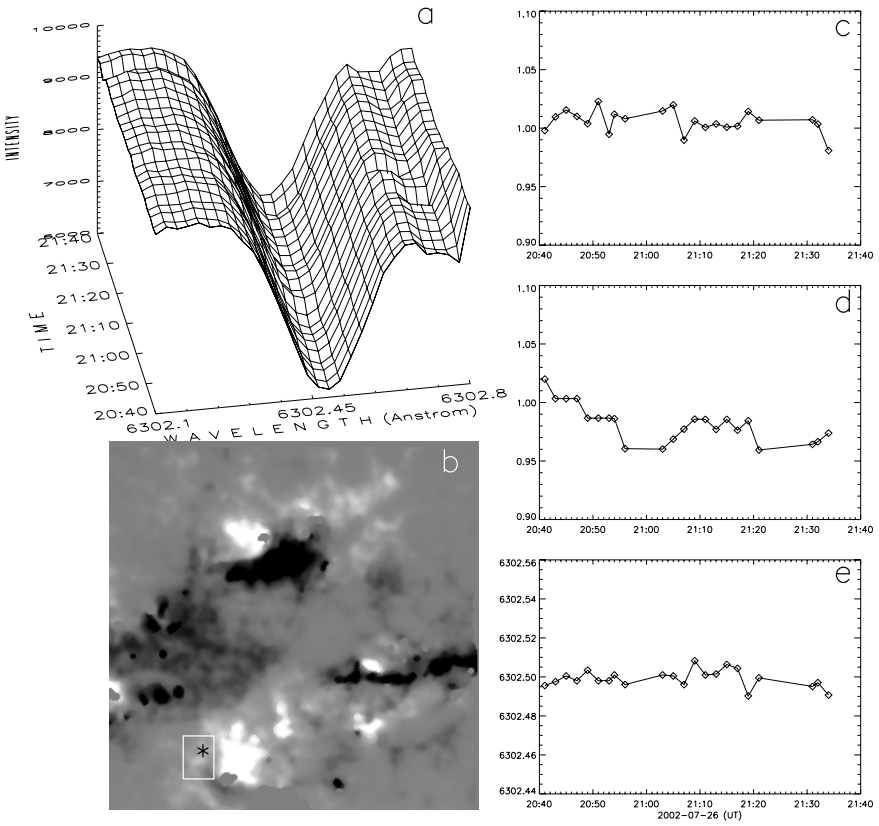

Fig. 5 (a) The evolution of line profiles from 20:41 to 21:36 UT at a sample point indicated by $*$ in the box of a sample longitudinal magnetogram observed with the IVM shown in Panel (b). This point is located in ribbon R3 of flare 2. (c)–(e). The time profiles for the width, depth and central wavelength of the line series in (a). The line width and depth are normalized with respect to the values of the non-flaring region.

some sudden changes associated with the second flare. The mean value of the positive magnetic field rapidly dropped nearly $\sim$5 G, while the mean absolute value of the negative field was rapidly enhanced $\sim$2 G. Again, the positive and negative flux changes were unbalanced. The magnitude of changes were small compared to that of some of the other sub-regions, but they are not negligible, since both positive and negative fluxes underwent sudden but permanent changes at the same time. The changes occurred at the starting time of the flare (within the 1 minute time resolution). It is worth mentioning that this kind of change is easily missed with the previous method that uses a larger region for flux integration (Wang et al. 2002) or the method by Sudol & Harvey (2005), who used the mean value of the magnetic field of every pixel for detection.

The second and third flares share a common magnetic polarity inversion line. Magnetic flux changes occur in box 44, crossing the polarity inversion line. However, the positive magnetic flux was enhanced for the second flare but decreased for the third flare; negative magnetic flux decreased for the second flare but increased for the third flare. In boxes 5 and 15, only the positive flux underwent

abrupt changes. In box 15, the mean magnetic field rapidly increased by ~ 10 G, but in box 4, the mean value rapidly decreased by ~ 10 G. The sudden flux changes in boxes 5 and 15 were about 2 minutes after the onset of flare 3 and lasted about 4 minutes. However, if we sum the magnetic fluxes in both boxes 5 and 15, no permanent flux change appears with this flare (Fig. 4h). The sudden disturbance in the flux curve of Figure 4h is apparently caused by flare ribbon emissions, and thus belongs to the class of "magnetic transients" (Zirin & Tanaka 1981; Patterson 1984; Kosovichev & Zharkova 2001). The changes in boxes 5 and 15 are very probably due to a sudden movement (or expansion) of the magnetic flux from box 5 to 15.

4 SUMMARY AND DISCUSSION

With an extensive analysis, we study the temporal evolution of magnetic flux during three successive M-class flares in two adjacent active regions. We divide the whole region into 10×10 sub-regions (boxes) and derive the time profile of magnetic flux in each sub-area. Each time profile is analyzed and compared with the timing and location of the flares. This method has the advantage of capturing flares' associated magnetic changes having smaller magnitude. For example, for the second flare, the average amplitude of change is only about 2–5 G. This kind of change is easily missed with conventional methods that use a larger region for flux integration (Wang et al. 2002) or the pixel averaging method (Sudol & Harvey 2005). This method allows us to find some additional areas with flare-associated magnetic changes, e.g., box 33 for the second flare and boxes 5 and 15 for the third flare. All flares analyzed in this paper are M-class flares. We see that abrupt magnetic changes are not only restricted to large X-class flares.

All changes occurred $1 \sim 10$ minutes after the starting times of the flares or at the starting times of the flares (within the one minute time resolution). This strongly indicates that the changes are consequences of solar flares. We can refer to the suggestion made by Wang et al. (2002) that the relaxation of the magnetic field causes the sunspot to expand. A sudden relaxation of the magnetic fields may cause the sunspot to expand quickly, thus causing sudden flux changes. A special example is the flux changes found in boxes 5 and 15. Magnetic expansions could happen from box 5 to box 15. Again, this kind of expansion-caused change could only be found with this extensive analysis.

Sometimes the temporal behavior of the flare-associated magnetic changes is gradual, such as in the second flare. This kind of change is quite different from the step-function-like changes reported in literature. We need more statistical study of this type of dynamic behavior.

It is commonly accepted that measurements of magnetic fields may be greatly affected by line profile changes and shifting of the line center. Based on simulations, Qiu & Gary (2003) showed that a magnetic anomaly is mainly caused by line reversal (from absorption to emission) and great line broadening during flares. The MDI instrument measures the line intensities at five positions along the spectral profile. Line intensities at four spectral positions separated by an interval of 0.075 Å are readout with respect to the left and right circular polarization modes. The intensities are then converted to the measured velocity and magnetic strength. Only the final results are returned from MDI, but the intermediate quantities, like the line intensities at five positions and the shift parameters, are not recorded once the computation is done (Scherrer et al. 1995; Qiu & Gary (2003)). With the aid of IVM data, we did not find any line reversal at the flaring sites. The changes of line width and depth are within 5%. The fluctuation of the line center is within ± 0.01 Å, corresponding to $\pm 0.5\,\mathrm{km\,s^{-1}}$. Only a large velocity field over $10\,\mathrm{km\,s^{-1}}$ generated by a flare energy release could cause false magnetic measurements (Qiu & Gary (2003)). Therefore, we conclude that the magnetic changes reported in this paper are not caused by line changes.

Acknowledgements The authors are grateful to the anonymous referee for improving the paper. We are grateful to the BBSO and IVM observing staff for their support. We are also grateful to the *RHESSI* team for providing *RHESSI* data and software. SOHO is an international cooperation project between ESA and NASA. This work was supported by National Natural Science Foundation

of China (Grants Nos. 10833007, 10933003 and 10928307), and by the National Basic Research Program of China (973 Program) under grant 2011CB811402.

References

Ding, M. D., Qiu, J., & Wang, H. 2002, ApJ, 576, L83
Hudson, H. S., Fisher, G. H., & Welsch, B. T. 2008, in Subsurface and Atmospheric Influences on Solar Activity, Astronomical Society of the Pacific Conference Series, Vol. 383, eds., R. Howe, R. W. Komm, K. S. Balasubramaniam, & G. J. D. Petrie , 221
Jefferies, J. T., & Mickey, D. L. 1991, ApJ, 372, 694
Kosovichev, A. G., & Zharkova, V. V. 2001, ApJ, 550, L105
LaBonte, B. J., Mickey, D. L., & Leka, K. D. 1999, Sol. Phys., 189, 1
Lin, R. P., Dennis, B. R., Hurford, G. J., et al. 2002, Sol. Phys., 210, 3
Mickey, D. L., Canfield, R. C., Labonte, B. J., et al. 1996, Sol. Phys., 168, 229
Patterson, A. 1984, ApJ, 280, 884
Qiu, J., & Gary, D. E. 2003, ApJ, 599, 615
Scherrer, P. H., Bogart, R. S., Bush, R. I., et al. 1995, Sol. Phys., 162, 129
Spirock, T. J., Yurchyshyn, V. B., & Wang, H. 2002, ApJ, 572, 1072
Sudol, J. J., & Harvey, J. W. 2005, ApJ, 635, 647
Tan, B., Ji, H., Huang, G., et al. 2006, Sol. Phys., 239, 137
Wang, H., & Liu, C. 2010, ApJ, 716, L195
Wang, H., Qiu, J., Jing, J., et al. 2004, ApJ, 605, 931
Wang, H., Spirock, T. J., Qiu, J., et al. 2002, ApJ, 576, 497
Wang, J., Zhao, M., & Zhou, G. 2009, ApJ, 690, 862
Zhao, M., Wang, J., Matthews, S., et al. 2009, Research in Astronomy and Astrophysics, 9, 812
Zhou, T., & Ji, H. 2009, Research in Astronomy and Astrophysics, 9, 323
Zirin, H., & Tanaka, K. 1981, ApJ, 250, 791